

Relations between structural distortions and transport properties in $\text{Nd}_{0.5}\text{Ca}_{0.5}\text{MnO}_3$ strained thin films.

E. Rauwel Buzin, W. Prellier*, B. Mercey, Ch. Simon and B. Raveau

Laboratoire CRISMAT, CNRS UMR 6508, 6 Bd du

Maréchal Juin, 14050 Caen Cedex, FRANCE.

(October 30, 2018)

Abstract

Strained thin films of charge/orbital ordered (CO/OO) $\text{Nd}_{0.5}\text{Ca}_{0.5}\text{MnO}_3$ (NCMO) with various thickness have grown on (100)- SrTiO_3 and (100)- LaAlO_3 substrates, by using the Pulsed Laser Deposition (PLD) technique. The thickness of the films influences drastically the transport properties. As the thickness decreases, the CO transition increases while at the same time the insulator-to-metal transition temperature decreases under application of a 7T magnetic field. Clear relationships between the structural distortions and the transport properties are established. They are explained on the basis of the elongation and the compression of the Mn-O-Mn and Mn-O bond angles and distances of the $Pnma$ structure, which modify the bandwidth and the Jahn-Teller distortion in these materials.

Typeset using REVTeX

*prellier@ismra.fr

I. INTRODUCTION

Perovskite type manganites such as $R_{1-x}A_xMnO_3$ (R=rare earth ion and A=alkaline earth ion) have been extensively investigated due their properties of colossal magnetoresistance (CMR)¹. The CMR effects originates from a competition between a ferromagnetic metallic (FMM) state and an antiferromagnetism insulating (AFMI) state. The appearance of the FMM state is explained by the double exchange (DE) mechanism², whereas the AFMI state originates from the Jahn-Teller (JT) distortions³⁻⁵, leading in the case of small A-site cations to the charge/orbital ordered (CO/OO) phenomenon⁶. The efforts made for understanding the magnetotransport properties of manganite thin films^{1,7,8} have shown that the physical properties are often different from the bulk materials. The main reason deals with the strains included the substrate-induced strains which modify the lattice parameters of the film and change the properties as shown recently for $Pr_{0.5}Ca_{0.5}MnO_3$ ⁹⁻¹¹, $La_{1-x}Ba_xMnO_3$ ¹² and $Nd_{0.5}Ca_{0.5}MnO_3$ ¹³.

In manganite thin films, the strains are susceptible to modify the Mn-O-Mn angles and Mn-O distances. Consequently, this affects the bandwidth and also the JT distortions, so that DE and CO/OO phenomena may be drastically influenced. Based on these considerations, the strain effects should decrease as the thickness increases and it should be possible to establish relationships between the structural distortions and the transport properties, by studying the properties of the films with various thicknesses.

Starting from $Nd_{0.5}Ca_{0.5}MnO_3$ films where a spectacular CMR effect was previously evidenced¹³, compared to the bulk¹⁴, we have carried out a systematic study of films with different thickness grown in situ using the Pulsed Laser Deposition technique (PLD) on both (100)-SrTiO₃ and (100)-LaAlO₃ substrates. In this paper, a clear correlation between the structural distortions and the transport properties (insulator-to-metal T_{IM} transition under a magnetic field, CO/OO T_{CO} transition). We suggested that for small films thickness the elongation of the Mn-O bonds prevails, reinforcing the JT distortion and consequently the CO/OO state, whereas for large thickness the flattening of the Mn-O-Mn bond angles

prevails, increasing the bandwidth favoring the insulator-to-metal transition to the detriment of the CO/OO state.

II. EXPERIMENTAL

Films with different thicknesses were deposited on single crystal substrates of (100)-SrTiO₃ (STO) and (100)-LaAlO₃ (LAO) from a dense targets of Nd_{0.5}Ca_{0.5}MnO₃ using the PLD technique. Detailed of the process can be found elsewhere¹³. The structural study was done by X-ray diffraction (XRD) using a Seifert XRD 3000P for the Θ -2 Θ scans and a Phillips MRD X'pert for the in-plane measurements (Cu K α , $\lambda=1.5406\text{\AA}$). The in-plane lattice parameters were obtained from the (103)_C reflection (where C refers to the ideal cubic perovskite cell, $a_C=3.9\text{\AA}$). An electron microscope JEOL 2010 equipped with an Energy Dispersive Spectroscopy (EDS) analysis, was used for the electron diffraction (ED) study. The EDS has shown that the cationic composition of the film is homogeneous and remains very close to the nominal one "Nd_{0.5±0.02}Ca_{0.5±0.02}MnO_x" within experimental error.

The resistivity (ρ) of the films was measured with a PPMS Quantum Design as a function of the magnetic field (H) and the temperature (T) using four-probe contacts. The thickness (t) of the films is measured using a Dektak³ST surface profiler.

Besides the classical growth parameters such as the deposition temperature, the oxygen pressure, we found that the energy of the laser was also important in order to obtain a single phase. The optimum energy value is $200mJ$ which corresponds to $2J/cm^2$ on the target. This is evidenced on Fig.1 for a 2000\AA thick film of NCMO on STO. A low ($132mJ$) or a high ($240mJ$) laser energy leads to a poor crystallization of the film with appearance of a secondary phase.

III. RESULTS

A. Structural properties

The structure of bulk NCMO is orthorhombic ($Pnma$) with $a = 5.4037\text{\AA}$, $b = 7.5949\text{\AA}$ and $c = 5.3814\text{\AA}$ ¹⁵. Some area of the film have been investigated by ED and we found that the films are single phase, [010]-oriented, i.e. with the [010]-axis perpendicular to the STO substrate plane, and [101]-oriented, i.e. with the [101]-axis perpendicular to the LAO substrate plane in the space group $Pnma$. This orientation is not surprising and resulting from the lattice mismatch between the film and the substrate as previously reported for $\text{Pr}_{0.5}\text{Ca}_{0.5}\text{MnO}_3$ thin films grown on (100)- SrTiO_3 and (001)- LaAlO_3 substrates^{9,10}. Details of the transmission electron microscopy study are currently undertaken and will be published elsewhere.

Fig.2a shows the evolution of the lattice parameters of the NCMO film grown on STO versus thickness. One observed that the in-plane lattice parameter d_{101} decreases as the thickness of the film increases while at the same time, the out-of-plane lattice parameter d_{020} increases. The lattice parameters of films on LAO were also determined (Fig.2b) but, due to the twins of this substrates, we were not able to obtain the in-plane lattice parameters. The out-of-plane lattice parameters are almost constant on LAO when the thickness is changing, suggesting that the film is quasi-relaxed even for small thickness.

B. Transport properties

Figure 3a shows the resistivity dependence of the temperature for NCMO films on STO. Without a magnetic field, all films present a semiconducting behavior with an anomaly around 275K, corresponding to the T_{CO} . A similar effect is observed on the bulk, but at a lower temperature close to 250K¹⁷. In fact, this anomaly in the $\rho(T)$ curves is more clear (inset of Fig. 3a), when the resistance is plotted in a logarithmic scale versus the inverse of the temperature. When applying a magnetic field of 7T, while the thinner film ($t = 670\text{\AA}$) remains insulating in the whole temperature range of 4-300K, the thicker films ($t >$

1340Å) show an insulator-to-metal transition (T_{IM}) at 100K and 130K for the 1340Å and 2000Å films respectively. Such an effect is typical of the metastability of the CO/OO state where a magnetic field (abbreviated H_C) can induce a metallic behavior at low temperature. However, the magnetic field required is much higher in the bulk compound (close to 20T for the same temperature)¹⁴. In fact, there is a dependence of the critical field with the temperature (Figure 3b). The resistivity shows an important decrease on a logarithmic scale at a critical field (H_C) indicating the field-induced melting of the CO/OO state. This field-induced insulator-to-metal transition, which accompanies the collapsing of the CO/OO state takes place below T_{CO} . This decrease can be viewed as a CMR of about four orders of magnitude at 75K. A clear hysteresis (between the lower and the upper critical fields) is seen at these temperatures as previously reported on several CO/OO compounds^{6,18,19} but this hysteretic region is more pronounced when the temperature is decreasing (see $\rho(H)$ at 25K in Fig.3b). In addition, the temperature dependence of the large hysteresis region is a feature of a first order transition and has been extensively studied for the composition $\text{Nd}_{0.5}\text{Sr}_{0.5}\text{MnO}_3$ in Ref.¹⁸. Note also the reentrant nature of the CO at 25K due to the fact that a 7T magnetic field is not enough to completely melt this state.

On LAO substrates, the $\rho(T)$ curves are practically similar (Fig.4a) to those on STO except that in this case, even the thinnest film (670Å) displays an insulator-to-metal transition when applying a magnetic field of 7T. Moreover, the T_{IM} is higher than in the case of STO which is consistent with the quasi-relaxed NCMO film found on LAO (for a 1340Å film, $T_{IM} < 100K$ on STO and $T_{IM} = 110K$ on LAO). Large hystereses indicating the first-order phase transition are also observed (Fig.4b) and, in the same way, there is an increase of the T_{CO} when the thickness of the film decreases (inset of Fig. 4a).

C. Discussion

This study shows that the thickness of NCMO films deposited on STO influences strongly the transport properties of the material. For the largest thickness ($t = 2000\text{Å}$), an insulator-

to-metal transition is induced under 7T in contrast to the bulk¹⁴, although the cell parameters reach values close to those of the bulk ceramics¹⁵. Moreover, the T_{IM} under 7T magnetic field decreased as the thickness decreases whereas at the same time, the T_{CO} increases so that for a small thickness ($t = 650\text{\AA}$) the film remains insulator.

Though it was suggested by several authors in bulk samples of the same composition that electronic phase separation can be at the origin of the drop in resistivity^{15,16}, no evidence of such phase separation was found in the thin films. We have indeed observed a continuous variation of the lattice parameters with the thickness of the films.

Thus, in order to explain this evolution, we have take into consideration the following features concerning the strains induced by the STO substrates

(i) The tensile stain along the [101] direction (in the plane of the substrate) can increases both the Mn-O-Mn angles and Mn-O distances in the equatorial plane (see Fig.5a). The increase of the Mn-O_{EQ}-Mn²⁰ bond angle increases the bandwidth²¹, the angles tending toward 180°, so that DE is involved. Consequently this structural effect should destabilize the CO/OO state and favor the T_{IM} . The increase of the Mn-O bond length induces the antagonist effect, favoring the distortion of the MnO₆ octahedra, i.e. the Jahn-Teller distortion, so that the CO/OO state should be stabilized.

(ii) The compression of the structure along the [010] direction (along the out-of-plane direction on STO), which appears simultaneously, results in a decrease of the Mn-O_{AX}-Mn²⁰ angle along this direction. Consequently, this decreases the bandwidth and stabilizes the CO/OO state.

(iii) In the *Pnma* structure (such as NCMO), there are eight Mn-O_{EQ}-Mn bonds against four Mn-O_{AX}-Mn bonds. Thus, the bandwidth along the Mn-O_{EQ} is consistently larger than the bandwidth along the Mn-O_{AX} direction which indicates that the DE along the [101] direction prevails over the [010] direction²¹.

(iv) Viewing these remarks, it is reasonable to assume that the substrate-induced strains modify in a first step the tilting of the octahedra, i.e. the Mn-O-Mn angles and only in a second step the Mn-O bond lengths in the plane of the substrate.

For the larger films thickness ($t > 2000\text{\AA}$), the cell parameters are close to those of the bulk leading consequently to a tilting of the octahedra rather than a modification of the bond lengths. In other words, the variation of the Mn-O-Mn angles prevails over the variation of the Mn-O distances. Thus, as d_{101} increases the Mn-O_{EQ}-Mn angles increases with respect to the bulk. In contrast, as d_{010} decreases the Mn-O_{AX}-Mn angle decreases, resulting in an increase of the bandwidth along the [101] direction and a decrease of the bandwidth along the [010] direction. But as pointed out above, the first effect prevails over the second one. As a consequence, the DE favored with respect to the bulk, so that the CO/OO state is less stable and an T_{IM} is obtained under a 7T magnetic field contrary to the bulk.

As the thickness of the film decreases from 2000 \AA , d_{101} increases significantly so the Mn-O_{EQ}-Mn bond angle reached 180° rapidly and the Mn-O_{EQ} bond length increases. The increase of the Mn-O_{EQ} distance induces a JT distortion of the octahedra, stabilizing the CO/OO state at the detriment of the T_{IM} transition. This explains why the T_{CO} transition increases as the thickness of the film decreases and the T_{IM} transition under 7T decreases correlatively. Finally, for the smaller film thickness ($t = 650\text{\AA}$), the d_{101} is very close to the STO parameter, and the bond angle Mn-O_{EQ} effects prevails over the Mn-O_{EQ}-Mn effect, so that the CO/OO state is the most stable. Note that the simultaneous decrease of the d_{010} , i.e. decrease of Mn-O_{AX}-Mn also favors the stabilization of the CO/OO state.

In the case of NCMO films grown on LAO, the substrate-induced strains lead in fact to rather similar effects. Indeed, one observes a compression along the [010]-axis in the plane of the substrate. As shown in Fig.5b, this induces a decreases of the Mn-O_{AX}-Mn angles and of the Mn-O_{AX} bond lengths similar to what occurs for STO; an increase of the Mn-O_{EQ}-Mn out-of-plane bond angle is induced, but in this case the increase of the Mn-O_{EQ} bond distance does not prevail over the Mn-O_{EQ}-Mn angle (not imposed by the substrate). For small thickness ($t = 650\text{\AA}$), the T_{IM} transition is favored with respect to the CO/OO state.

IV. CONCLUSION

In conclusion, we grown high quality thin films of $\text{Nd}_{0.5}\text{Ca}_{0.5}\text{MnO}_3$ on SrTiO_3 and LaAlO_3 using the PLD technique. We have shown that we are able to induce an insulator-to-metal transition at a magnetic field much lower than the corresponding bulk compound by the modification of the structure through the utilization of the appropriate substrate. Moreover the substrate-induced strains increases the $\text{Mn-O}_{EQ}\text{-Mn}$ bond angles on both LAO and STO substrates (even if the orientation of the film is different) favoring the double exchange and consequently destabilizing the charge/orbital state leading to a decrease of the critical magnetic field as compared to the bulk.

REFERENCES

- ¹ R. Von helmolt, J. Wecker, R. Holzapfel, L. Schultz, and K. Samwer, Phys. Rev. Lett. 71, 2331 (1993), McCormack, S. Jin, T. Tiefel, R. M. Fleming, J.M. Philips, and R. Ramesh, Appl. Phys. Lett. 64, 3045 (1994).
- ² C. Zener, Phys. Rev. 82, 403 (1951).
- ³ A.J. Millis, P.B. Littlewood and B. Shraiman, Phys. Rev. Lett. 74, 5144 (1995).
- ⁴ EO. Wollan and W.C. Koehler, Phys. Rev. 100, 545 (1955).
- ⁵ J.B. Goddenough, Phys. Rev. 100, 564 (1955).
- ⁶ for a review see: C.N.R. Rao, A. Arulraj, A.K. Cheetham and B. Raveau, J. Phys. Condens. Mater. 12, R83 (2000).
- ⁷ T. Vankatesan, M. Rajeswari, Z.-W. Dong, S.B.Ogale, and Ramesh, Philos. Trans. R. Soc. London 356, 1661 (1998), W. Prellier, Ph. Lecoeur and B. Mercey, J. Phys. Condens. Mater. 13, R915 (2001).
- ⁸ K. Chahara, T. Ohno, M. Kasai, and Y. Kosono Appl. Phys. Lett. 63, 1990 (1993).
- ⁹ W. Prellier, A. M. Haghiri-Gosnet, B. Mercey, Ph. Lecoeur, M. Hervieu, Ch. Simon, and B. Raveau, Appl. Phys. Lett. 77, 1023 (2000).
- ¹⁰ A.M. Haghiri-Gosnet, M. Hervieu, Ch. Simon, B. Mercey, and B. Raveau, J. of Appl. Phys. 88, 3545 (2000).
- ¹¹ W. Prellier, Ch. Simon, A. M. Haghiri-Gosnet, B. Mercey, and B. Raveau, Phys. Rev. B 62, R16337 (2000).
- ¹² J. Zhang, H. Tanaka, T. Kanki, J. Choi and T. Kawai, Phys. Rev. B 64, 184404 (2001).
- ¹³ E. Rauwel Buzin, W. Prellier, Ch. Simon, S. Mercone, B. Mercey and B. Raveau, Appl. Phys. Lett. 79, 647 (2001).

- ¹⁴ M. Tokunaga, N. Miura, Y. Tomioka, Y. Tokura, Phys. Rev. B 57, 5259 (1998).
- ¹⁵ F. Millange, S. de Brion and G. Chouteau, Phys Rev. B 62, 5619 (2000).
- ¹⁶ P. Murugavel, C. Narayana, A.K. Sood, S. Parashar, A.R. Raju and C.N.R. Rao, Europhys. Lett. 52, 961 (2000).
- ¹⁷ M. Respaud, A. Llobet, C. Frontera, C. Ritter, J.M. Broto, H. Rakoto, M. Goiran, J.L. García-Muñoz, Phys. Rev. B 61, 9014 (2000).
- ¹⁸ H. Kuwahara, Y. Tomioka, A. Asamitsu, Y. Moritomo, Y. Tokura, Science 270, 961 (1995).
- ¹⁹ Y. Tomioka *et al.*, Phys. Rev. B 53, R1689 (1996).
- ²⁰ O_{EQ} and O_{AX} refer respectively to the equatorial and axial oxygen (see. Figs. 4a-4b).
- ²¹ P.M. Woodward, T. Vogt, D.E. Cox, A. Arulraj, C.N.R. Rao, P. Karena and A.K. Cheetham, Chem. Mater. 10, 3652 (1998), A. Arulraj, P.N. Santhosh, R.S. Gopalan, A. Guha, A K Raychaudhuri, N. Kumar and C.N.R. Rao, J. Phys.: Condens. Mater 10, 8497 (1998).

Figures Captions:

Fig.1: Room temperature XRD in the range $40\text{-}55^\circ$ of a 2000\AA NCMO film on STO grown with various energy of the laser beam.

Fig.2: : (a): Evolution of the lattice parameters of NCMO on STO as a function of the thickness. (b): Evolution of the out-of-plane lattice parameters of NCMO on LAO as a function of the thickness The values of the bulk are indicated as a dot line (see text for details). Lines are only guide for the eyes.

Fig.3: NCMO films on STO with various thickness. (a): $\rho(T)$ under 0T (empty symbols) and 7T (full symbols). The inset depicts the evolution of the logarithmic resistivity versus the inverse of the temperature under 0T (empty symbols) and 7T (full symbols). Note the anomaly associated to the T_{CO} (marked by arrow). (b): $\rho(H)$ at various temperature for a 2000\AA film.

Fig.4: NCMO films on LAO with various thickness. (a): $\rho(T)$ under 0T (empty symbols) and 7T (full symbols). The inset depicts the Evolution of the logarithmic resistivity versus the inverse of the temperature under 0T (empty symbols) and 7T (full symbols). Note the anomaly associated to the T_{CO} (marked by arrow). (b): $\rho(H)$ at various temperature for a 2000\AA film.

Fig.5a: Idealized [010] NCMO structure on STO. The directions of the stress are indicate by arrows. F and S refer to the film and to the substrate.

Fig.5b: Idealized [101] NCMO structure on LAO. The directions of the stress are indicate by arrows. F and S refer to the film and to the substrate.

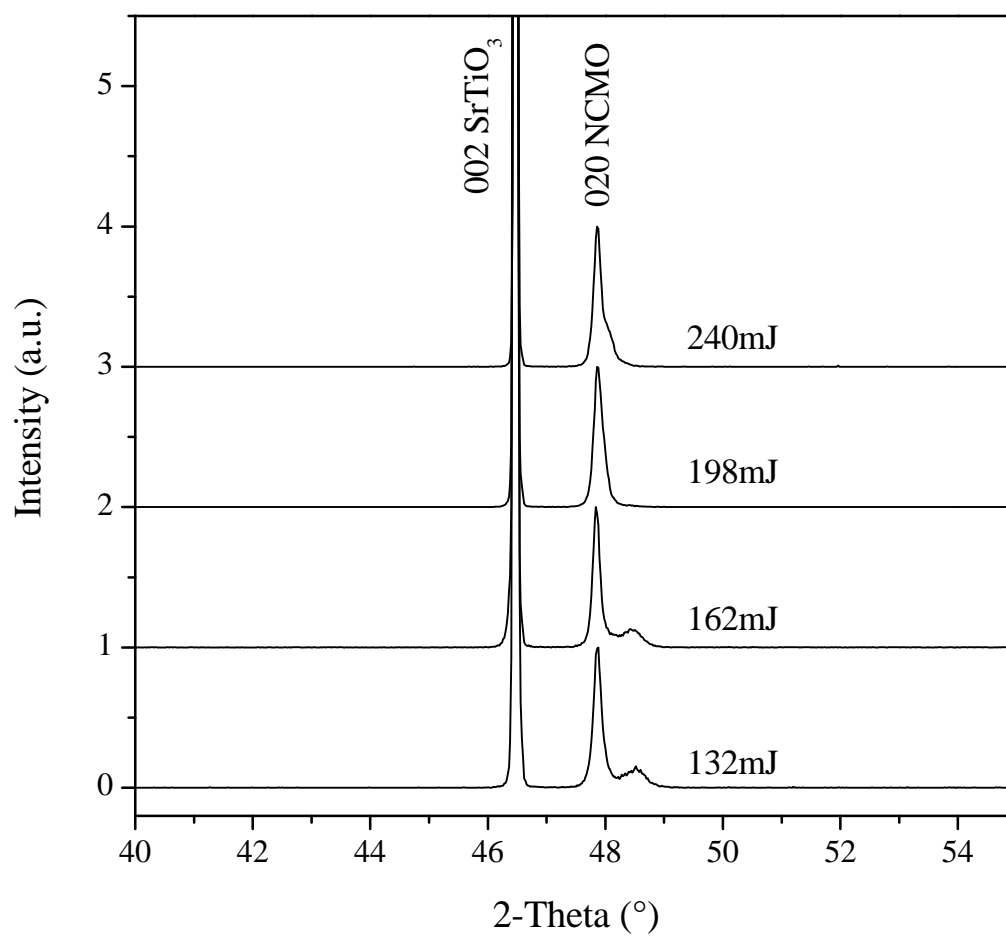


Figure 1

E. Rauwel Buzin et al.

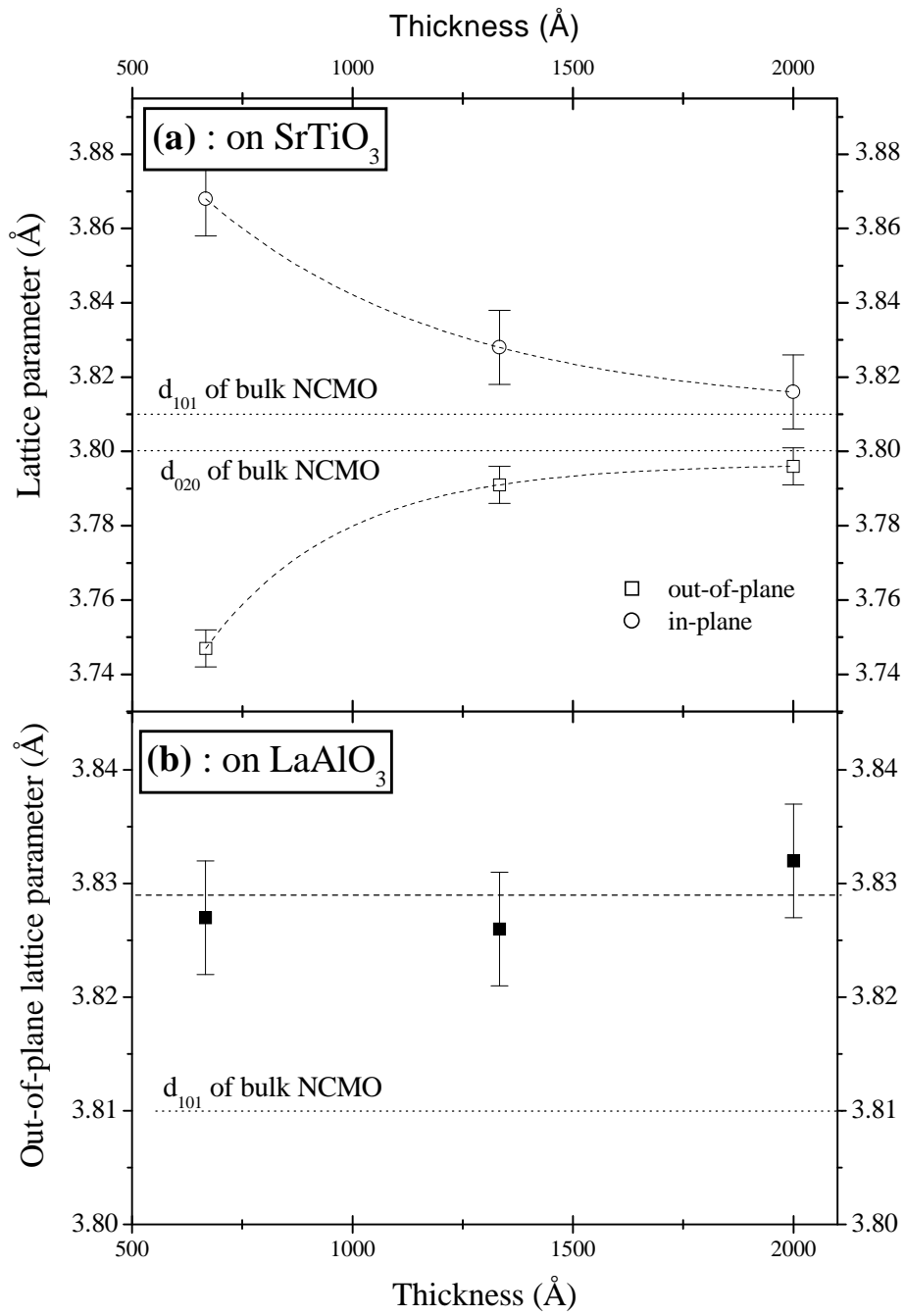


Figure 2

E. Rauwel Buzin et al.

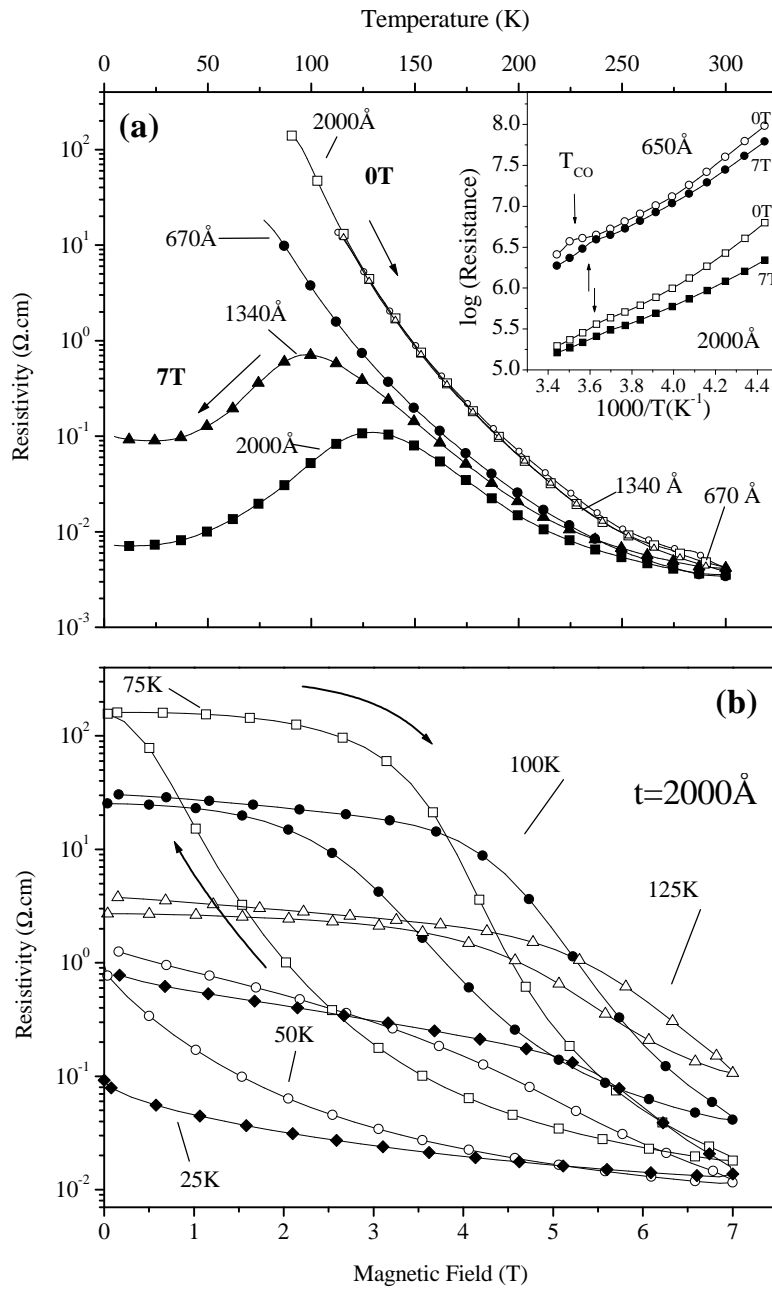


Figure 3

E. Rauwel Buzin et al.

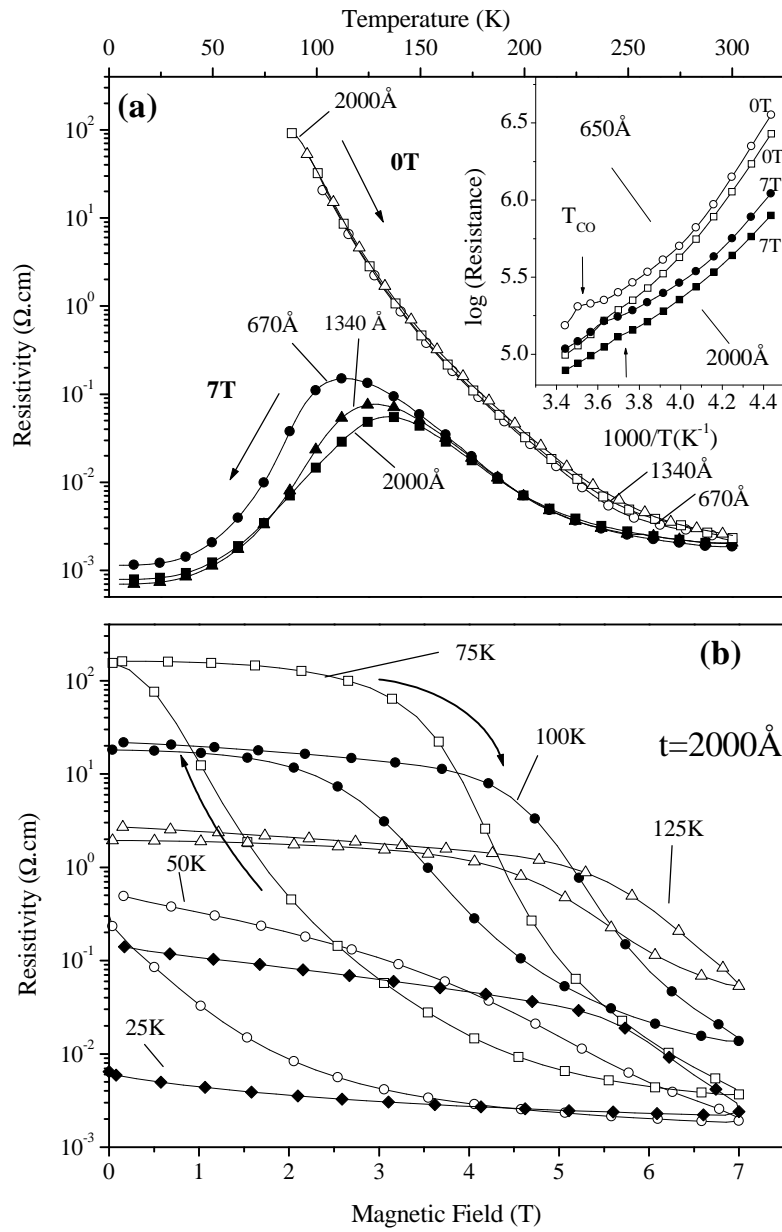


Figure 4

E. Rauwel Buzin et al.

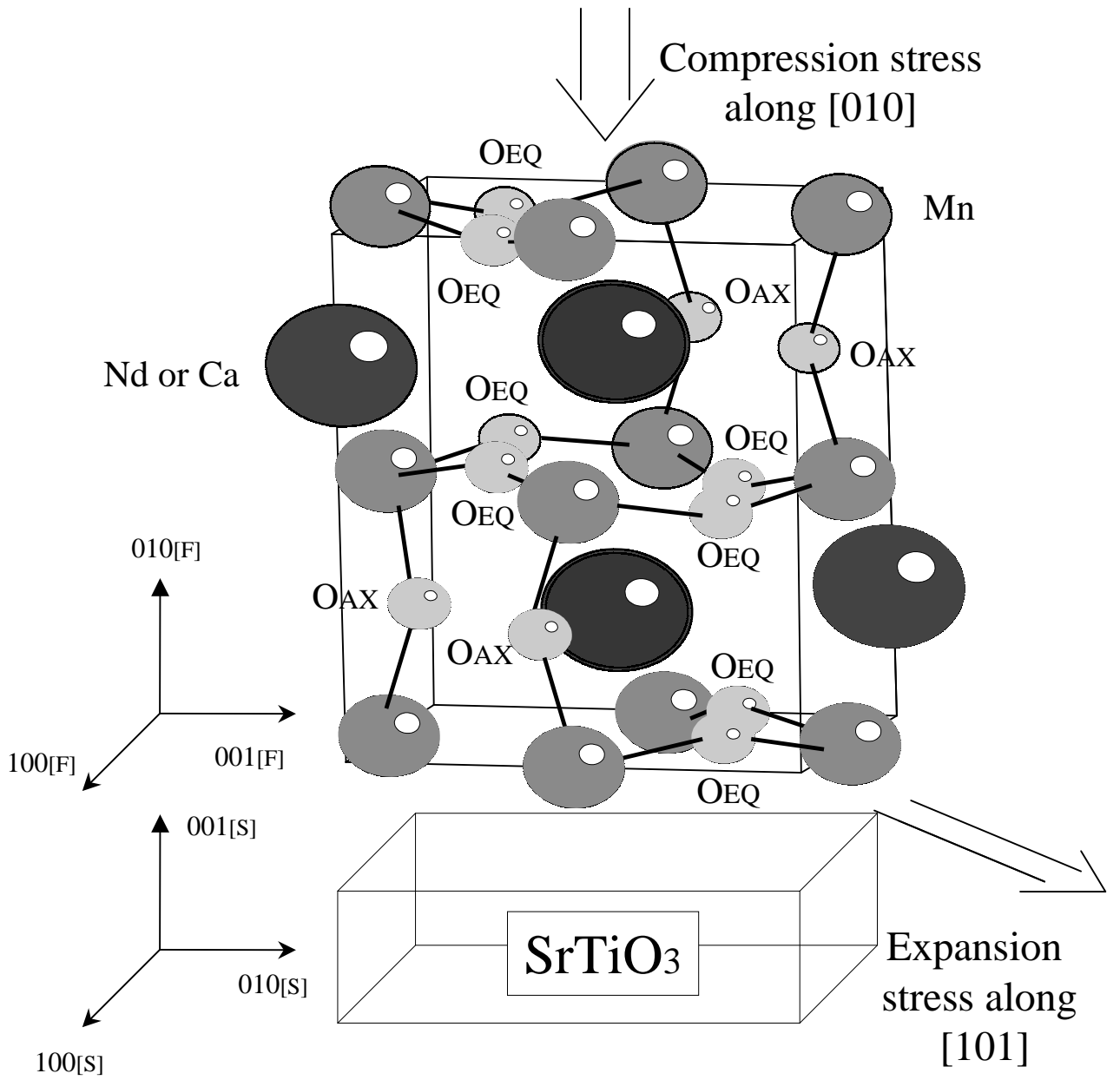


Figure 5a

E. RAUWEL BUZIN et al.

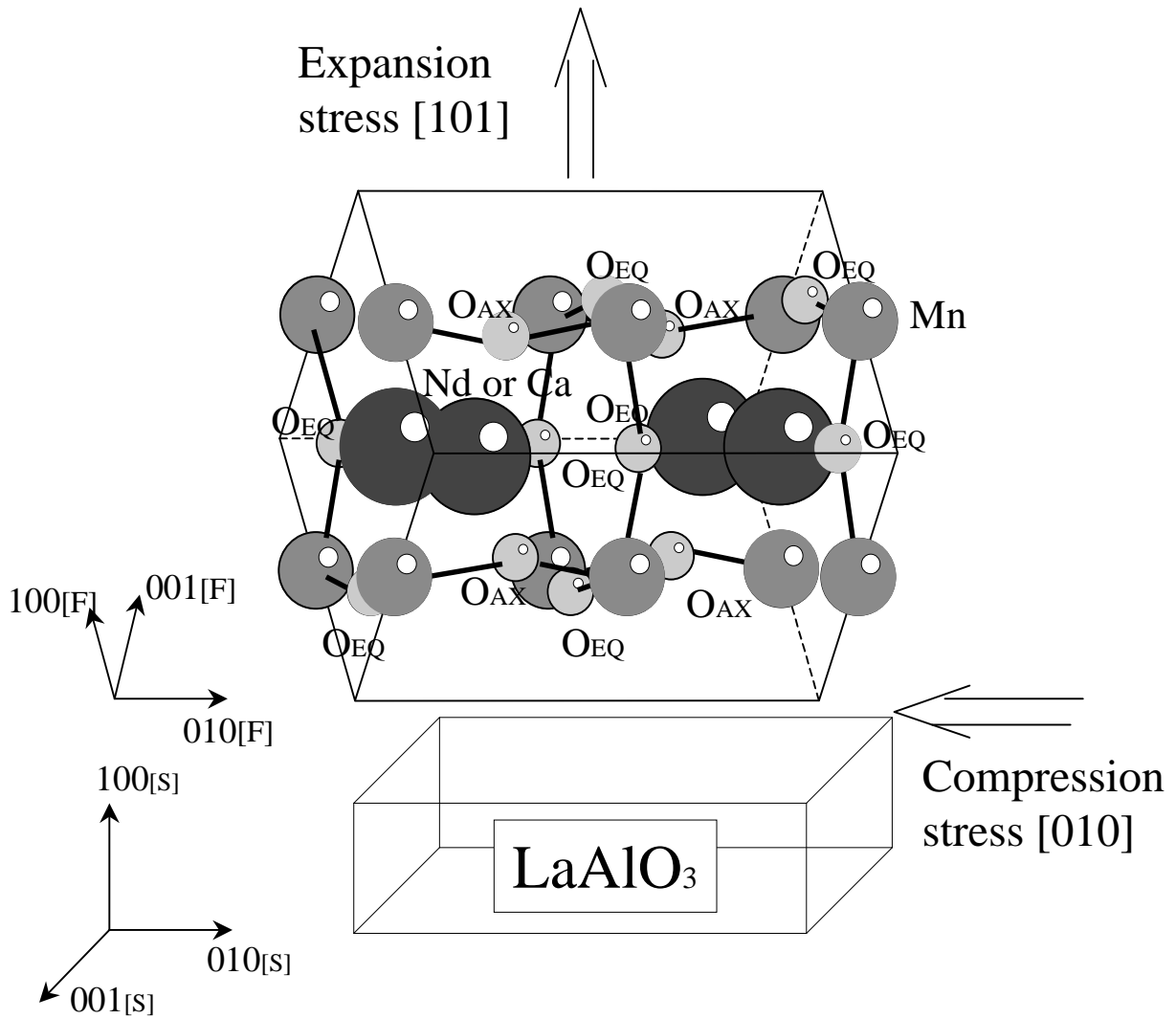


Figure 5b

E. RAUWEL BUZIN et al.